

# Secrecy Outage Analysis of Mixed RF-FSO Systems With Channel Imperfection

Volume 10, Number 3, June 2018

Hongjiang Lei, *Member, IEEE*

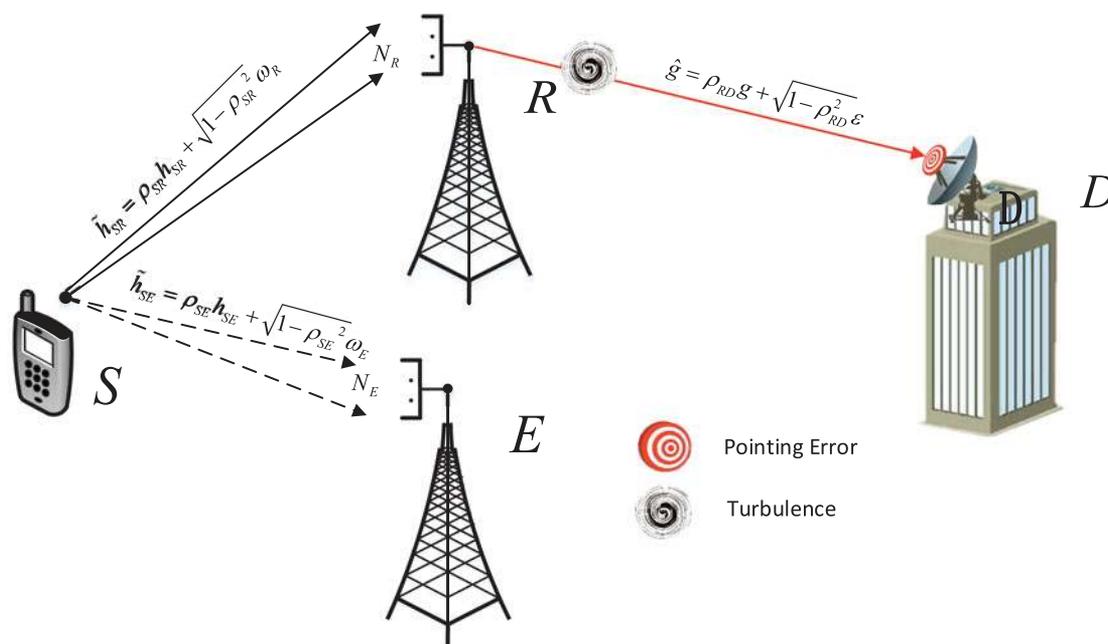
Haolun Luo

Ki-Hong Park, *Member, IEEE*

Zhi Ren

Gaofeng Pan, *Member, IEEE*

Mohamed-Slim Alouini, *Fellow, IEEE*



DOI: 10.1109/JPHOT.2018.2835562

1943-0655 © 2018 IEEE

# Secrecy Outage Analysis of Mixed RF-FSO Systems With Channel Imperfection

Hongjiang Lei <sup>1,2</sup> *Member, IEEE*, Haolun Luo,<sup>1</sup>  
Ki-Hong Park <sup>2</sup> *Member, IEEE*, Zhi Ren,<sup>1</sup>  
Gaofeng Pan <sup>3</sup> *Member, IEEE*,  
and Mohamed-Slim Alouini <sup>2</sup> *Fellow, IEEE*

<sup>1</sup>Chongqing Key Lab of Mobile Communications Technology, Chongqing University of Posts and Telecommunications, Chongqing 400065, China

<sup>2</sup>CEMSE Division, King Abdullah University of Science and Technology, Thuwal 23955-6900, Saudi Arabia

<sup>3</sup>Chongqing Key Laboratory of Nonlinear Circuits and Intelligent Information Processing, Southwest University, Chongqing 400715, China

DOI:10.1109/JPHOT.2018.2835562

1943-0655 © 2018 IEEE. Translations and content mining are permitted for academic research only. Personal use is also permitted, but republication/redistribution requires IEEE permission. See [http://www.ieee.org/publications\\_standards/publications/rights/index.html](http://www.ieee.org/publications_standards/publications/rights/index.html) for more information.

Manuscript received April 17, 2018; revised May 3, 2018; accepted May 8, 2018. Date of publication May 14, 2018; date of current version June 4, 2018. This work was supported in part by the National Natural Science Foundation of China under Grant 61471076, in part by the Chinese Scholarship Council under Grant 201607845004, in part by the Program for Changjiang Scholars and Innovative Research Team in University under Grant IRT\_16R72, in part by the special fund for Key Lab of Chongqing Municipal Education Commission, in part by the Project of Fundamental and Frontier Research Plan of Chongqing under Grants cstc2015jcyjBX0085 and cstc2017jcyjAX0204, and in part by the Scientific and Technological Research Program of Chongqing Municipal Education Commission under Grants KJ1600413 and KJ1704088. Corresponding author: Hongjiang Lei (e-mail: leihj@cqpt.edu.cn).

**Abstract:** We analyze the secrecy outage performance of a mixed radio frequency-free space optical (RF-FSO) transmission system with imperfect channel state information (CSI). We deal with a single-input multiple-output wiretap model, where a base station (works as the relay) forwards the signal transmitted from a user (source) to a data center (works as the destination), while an eavesdropper wiretaps the confidential information by decoding the received signal. Both the relay and the eavesdropper are armed with multiple antennas, and maximal ratio combining scheme is utilized to improve the received signal-to-noise ratio (SNR). The effects of imperfect CSI of the RF link and the FSO link, misalignment, detection schemes, and relaying schemes on the secrecy outage performance of mixed RF-FSO systems are studied. First, the cumulative distribution function and probability density function of FSO links with pointing error and two different detection technologies are derived. Then, we derive the closed-form expressions for the lower bound of the secrecy outage probability (SOP) with fixed-gain relaying and variable-gain relaying schemes. Furthermore, asymptotic results for the SOP are investigated by exploiting the unfolding of Meijer's  $G$ -function when the electrical SNR of FSO link approaches infinity. Finally, Monte Carlo simulation results are presented to corroborate the correctness of the analysis.

**Index Terms:** Physical layer security, imperfect channel state information (CSI), mixed radio frequency-free space optical (RF-FSO) systems, secrecy outage probability (SOP).

## 1. Introduction

As the number of wireless devices and systems has grown exponentially over the last several decades, spectrum scarcity became more and more severe. It has been struggled to find new available frequency bands (such as W-band) or new technologies (such as cognitive radio, non-orthogonal multiple access) to improve the spectral efficiency. Li *et al.* proposed new solutions to provide large-capacity and long-distance wireless transmission at W-band and the experimental results were demonstrated in [1], [2]. Furthermore, they designed a new high spectral efficiency fiber-wireless-integration (FWI) transmission system, which can realize multi-band delivery over the wire and wireless links in [3]. The mixed radio frequency-free space optical (RF-FSO) transmission systems are considered as a robust and efficient FWI system in practical communications networks since they combine the advantages of the RF and the FSO communication technologies [4], [5]. Recently, there are many literatures focusing on the mixed RF-FSO systems. The outage probability (OP) of mixed RF-FSO systems was investigated in [6]. The OP, average symbol error rate (ASER), and ergodic capacity (EC) of mixed RF-FSO systems with pointing error were studied in [7]. The new analytical expressions of the OP and average bit error rate for a dual-hop mixed RF/FSO relaying system were derived in [8]–[10], in which the RF link was assumed to experience Nakagami- $m$ ,  $\eta - \mu$ ,  $\kappa - \mu$ , and generalized Gamma distributions, respectively. The performance of mixed systems with a direct RF link between the source and the destination was investigated in [11], in which FSO and RF links experience double generalized Gamma and Nakagami- $m$  model, respectively. In addition, FSO links in mixed systems were subject to  $\mathcal{M}$ -distribution [12]–[15] and exponentiated Weibull distribution [16], respectively. The more information about mixed RF-FSO systems can be discovered in Table I in [11].

It is noteworthy that the performance analysis in previous works are limited since it is assumed that perfect channel state information (CSI) of the RF link and the FSO link are attainable at relay and destination node, respectively. Generally, CSI is estimated at the destination by transmitting a pilot signal and sent back to the source with a feedback link (if available). In practical wireless communication systems, it is impossible to obtain CSI without estimation errors. Furthermore, wireless channels change too rapidly to obtain perfect CSI at the source. Similarly, it is impossible to obtain the perfect CSI since the FSO link are vulnerable to atmospheric turbulence-induced fading and sensitivity to weather conditions, e.g., fog, snow, and rain. The mixed dual-hop systems with outdated CSI of RF link were recently investigated in [17]–[22] and the closed-form expressions for OP, average bit error probability (ABEP), and EC were obtained, respectively. But it was assumed that perfect CSI of FSO links were known in all these works. Feng *et al.* derived the probability density function (PDF) and cumulative distribution function (CDF) of FSO link with imperfect CSI with IM/DD and obtained the closed-form expressions for the OP, ABEP and EC in terms of Meijer's  $G$ -function in [23]. In this work, we consider the mixed RF-FSO systems with imperfect CSI for both the RF link and the FSO link.

Physical layer security has been regarded as a prospective safeguard technology for wireless communications because of the inherent randomness of wireless medium [24]. In recent years, several endeavors have been carried on to examine the secrecy performance of mixed RF-FSO systems [25]–[27]. The security reliability trade-off of mixed RF-FSO systems was studied in [25] and the closed-form expressions for OP, ASER, EC, and intercept probability were obtained. The effect of RF co-channel interference on the secure mixed systems was studied in [26]. The physical layer security of mixed RF-FSO systems was analyzed in [27], the closed-form expressions for secrecy outage probability (SOP) and ergodic secrecy capacity were attained under different relaying schemes and detection techniques. Obviously, one can see that all these works are based on perfect CSI at both the source and the relay.

As far as we know, there is no open literature studying the secrecy performance of mixed RF-FSO systems with imperfect CSI for RF or FSO link. From a practical standpoint, it is significant to analyze the effect of outdated CSI in various propagation conditions on the mixed system with different relaying schemes and detection techniques.

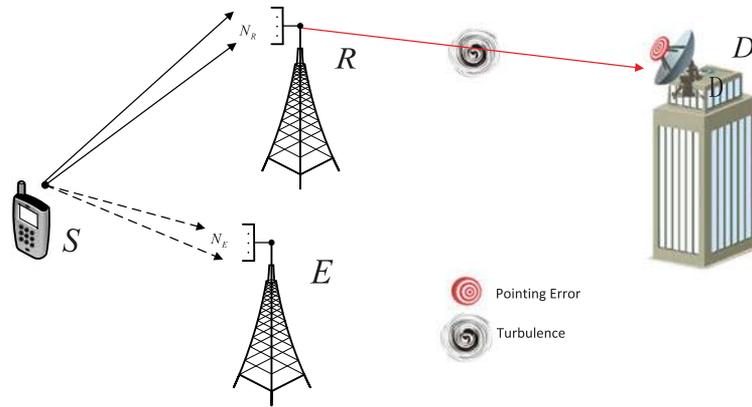


Fig. 1. The mixed RF-FSO systems that consist of a source ( $S$ ), a relay ( $R$ ), a destination ( $D$ ), and an eavesdropper ( $E$ ). Both  $R$  and  $E$  are equipped with multiple antennas and the CSI for all the links are imperfect.

We summarize the main contributions of this work as follows:

- In the last decades, the mixed RF-FSO systems with imperfect CSI for RF links were investigated in many literature, such as [17]–[22]. In all these works, it is assumed that the CSI of FSO link is perfect. Few works studied the FSO systems with the imprecise channel model, except [23]. But only the general performance metrics, such as the OP, ABEP and EC was studied in [23]. Based on the open literature and to the best of the authors' knowledge, there is no open literature simultaneously studied the mixed RF-FSO systems with imperfect CSI for both the RF link and the FSO link, even for the general performance metrics.
- The effects of imperfect CSI for the RF link and the FSO link, misalignment, different detection schemes, and multi-antenna techniques on secrecy outage performance are investigated. Firstly, the CDF and PDF of FSO links with pointing error and two different detection technologies are derived. Then we study the secrecy outage performance of mixed RF-FSO systems over Rayleigh and Gamma-Gamma channels, in which both fixed-gain and variable-gain relaying schemes, zero boresight misalignment, and direct/heterodyne detection techniques are considered. The closed-form expressions for lower bound SOP and asymptotic SOP are acquired and verified by the simulation results.
- Relative to [27], the multiple antennas are equipped at both the relay and the eavesdropper and maximal ratio combining (MRC) scheme is utilized to enhance the received signal-to-noise ratio (SNR). Furthermore, more practical scenarios are considered in which imperfect CSI is assumed for both the RF and the FSO link.

## 2. Channel and System Models

As illustrated in Fig. 1, we consider a mixed RF-FSO system that is composed of a source ( $S$ ) and destination ( $D$ ) armed with a single antenna, a relay ( $R$ ) armed with  $N_R$  antennas, and an eavesdropper ( $E$ ) armed with  $N_E$  antennas. MRC scheme is utilized at  $R$  and  $E$  to improve the received SNR. It is assumed that the RF and the FSO link are modeled as independent quasi-static Rayleigh and Gamma-Gamma fading channel, respectively. We considered that the CSI of both the RF link and the FSO link are outdated.

The RF channel fading coefficient with estimation error is given by

$$\tilde{h}_{Si,u} = \rho_{Si} h_{Si,u} + \sqrt{1 - \rho_{Si}^2} \omega_u, \quad (1)$$

where  $i \in \{R, E\}$ ,  $u = 1, \dots, N_i$ ,  $h_{Si,u}$  is the perfect channel coefficient between  $S$  and the  $u$ th antenna at destinations,  $\rho_{Si}$  denotes the correlation coefficient that is a constant that determines the accuracy of the RF channel model and  $0 \leq \rho_{Si} \leq 1$ , and  $\omega_u$  is a complex Gaussian random variable (RV) with

zero mean and the same variance of  $h_{Si,u}$ , which is used to model the channel estimation errors over RF links [28]. The received SNR at the  $u$ th antenna at  $i$  ( $i \in \{D, E\}$ ) can be expressed as

$$\gamma_{Si,u} = \frac{P_S}{N_0} |\tilde{h}_{Si,u}|^2, \quad (2)$$

where  $P_S$  is the transmit power at the source and  $N_0$  is the variance of additive white Gaussian noise (AWGN).

It is assumed that MRC scheme is applied at  $i$  ( $i \in \{R, E\}$ ), then the PDF and CDF of  $\gamma_{Si} = \frac{P_S}{N_0} \sum_{u=1}^{N_k} |\tilde{h}_{Si,u}|^2$  are given by [29]–[31]

$$f_{\gamma_{Si}}(\gamma) = \sum_{p=1}^{N_i} \frac{A_i}{\Gamma(p) \lambda_{Si}^p} \gamma^{p-1} \exp\left(-\frac{\gamma}{\lambda_{Si}}\right), \quad (3)$$

$$F_{\gamma_{Si}}(\gamma) = 1 - \sum_{p=1}^{N_i} \sum_{s=0}^{p-1} \frac{A_i}{\lambda_{Si}^s s!} \gamma^s \exp\left(-\frac{\gamma}{\lambda_{Si}}\right), \quad (4)$$

respectively, where  $A_i = \frac{(N_i-1)!}{(p-1)!(N_i-p)!} (1 - \rho_{Si})^{N_i-p} \rho_{Si}^{p-1}$  and  $\lambda_{Si}$  is the average SNR.

The imperfect FSO link channel coefficient is expressed as

$$\hat{g} = \rho_{RD} g + \sqrt{1 - \rho_{RD}^2} \varepsilon, \quad (5)$$

where  $g$  is the accurate channel coefficient of Gamma-Gamma channels,  $\rho_{RD}$  denotes the constant correlation coefficient, and  $\varepsilon$  means the channel estimation errors over FSO link. Differing from RF links, the channel estimation errors over FSO links are real, which means  $\varepsilon$  is a Gaussian RV. In this work, it is assumed that  $\varepsilon$  has zero-mean and unit variance and independent of  $g$ .

The CDF of imperfect receiver irradiance over FSO link with pointing error is given by [23]

$$F_{\hat{g}}(z) = \begin{cases} \zeta \sum_{k=0}^{\infty} \tau_k G_{1,2}^{1,1} \left[ \frac{1}{2(1-\rho_{RD}^2)} z^2 \middle| \begin{matrix} 1 \\ \nu_{k,0} \end{matrix} \right], & z > 0 \\ 1 - Z_0^{\text{PE}}, & z = 0 \end{cases}, \quad (6)$$

where  $\zeta = \frac{\xi^2}{\Gamma(a)\Gamma(b)\pi^{1.5}}$ ,  $\tau_k = \frac{2^{k+a+b-4} G_{2k}}{k!}$ ,  $G_{2k} = G_{6,3}^{1,6} \left[ \left( \frac{\xi^2+1}{ab\xi^2} \right)^2 \frac{8\rho_{RD}^2}{1-\rho_{RD}^2} \middle| \begin{matrix} \Delta(2,1-\xi^2), \Delta(2,1-a), \Delta(2,1-b) \\ \frac{k}{2}, \Delta(2,-\xi^2) \end{matrix} \right]$ ,  $\Delta(k, a) = \left[ \frac{a}{k}, \frac{a+1}{k}, \dots, \frac{a+k-1}{k} \right]$ ,  $a$  and  $b$  are the parameters of Gamma-Gamma fading models,  $\xi$  is the parameter of misalignment,  $\nu_k = \frac{k+1}{2}$ ,  $Z_0^{\text{PE}} = \frac{\xi^2}{\Gamma(a)\Gamma(b)\pi^{1.5}} \sum_{k=0}^{\infty} \frac{2^{k+a+b-4} G_{2k}}{k!} \Gamma\left(\frac{k+1}{2}\right)$  [23], where  $\Gamma(\cdot)$  is Gamma function, as defined by (8.310) of [32],  $G_{p,q}^{m,n}[\cdot]$  is the Meijer's  $G$ -function, as defined by (9.301) of [32].

The expression of the CDF in (6) contains the infinite series of summation which results from the use of the Maclaurin series for the exponential function. From (A.5) of [23], it can be found that only correlation coefficient influences the convergence rate of infinite series expressions. To evaluate the truncation errors, we define  $\text{MSE} = E \left[ (F_{\text{sim}}(z) - F_{\text{app}}(z))^2 \right]$ , where  $F_{\text{sim}}(z)$  and  $F_{\text{app}}(z)$  mean the simulation CDF and approximate CDF with  $N$  summation terms, respectively. Fig. 2 presents the MSE versus  $N$  for different  $\rho_{RD}$ . We can find that, for a given value of  $\rho_{RD}$ , the infinite summation is convergent with a finite truncation due to the characteristics of the exponential function. It can also observe that the convergence rate for a small  $\rho_{RD}$  is much faster than the one for a larger  $\rho_{RD}$ .

The relationship between the instantaneous SNR and the channel gain is expressed as [33]

$$\gamma_{RD} = \lambda_{RD} \hat{g}^r, \quad (7)$$

where  $\lambda_{RD} = \frac{\eta_e}{N_0}$ ,  $\eta_e$  is the effective photoelectric conversion ratio,  $N_0$  signifies the AWGN sample,  $r = 1$  denotes heterodyne detection (HD) and  $r = 2$  denotes with intensity modulation with direct

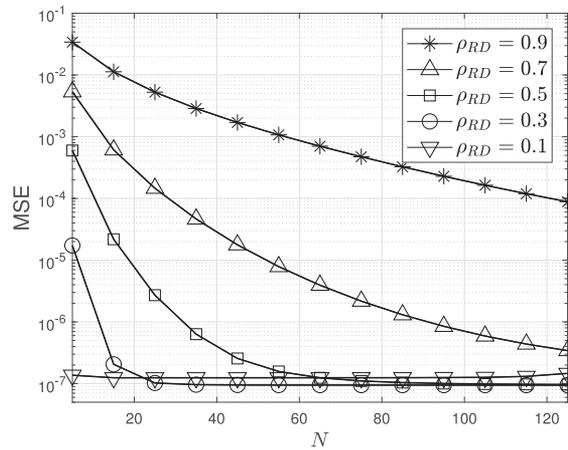


Fig. 2. The MSE versus  $N$  for different  $\rho_{RD}$ .

detection (IM/DD). Then the CDF and PDF of  $\gamma_{RD}$  are easily obtained as

$$F_{\gamma_{RD}}(\gamma) = \begin{cases} \zeta \sum_{k=0}^N \tau_k G_{1,2}^{1,1} \left[ \mu \gamma^{\frac{2}{r}} \middle| 1_{\nu_k, 0} \right], & \gamma > 0 \\ 1 - Z_0^{\text{PE}}, & \gamma = 0 \end{cases}, \quad (8)$$

$$f_{\gamma_{RD}}(\gamma) = \begin{cases} \zeta \sum_{k=0}^N \varphi_k \gamma^{\frac{k+1}{r}-1} \exp(-\mu \gamma^{\frac{2}{r}}), & \gamma > 0 \\ 1 - Z_0^{\text{PE}}, & \gamma = 0 \end{cases}, \quad (9)$$

respectively, where  $\mu = \frac{\lambda_{RD}^{-\frac{2}{r}}}{2(1-\rho_{RD}^2)}$  and  $\varphi_k = \frac{2^{k+a+b-3} \mu^{\nu_k}}{rk!} G_{2k}$ .

### 2.1 Fixed-Gain Relaying

If the CSI of  $S-R$  link are not available at  $R$ , then the simple method for  $R$  is just amplifying the signal with fixed gains and forwarding it to  $D$ . This method is also called as “blind” relaying scheme since the relay do not need instantaneous CSI of  $S-R$  link [34]. The received SNR at  $D$  with this scheme is given as [34]

$$\gamma_{eq}^F = \frac{\gamma_{SR} \gamma_{RD}}{\gamma_{RD} + C}, \quad (10)$$

where  $C$  is a constant.

The CDF of  $\gamma_{eq}^F$  is capable of being obtained as

$$\begin{aligned} F_{\gamma_{eq}^F}(\gamma) &= \int_0^\infty \Pr \left\{ \frac{\gamma_{SR} \gamma_{RD}}{\gamma_{RD} + C} < \gamma \middle| \gamma_{RD} \right\} f_{\gamma_{RD}}(\gamma_{RD}) d\gamma_{RD} \\ &= \int_0^\infty \Pr \left\{ \gamma_{SR} < \frac{\gamma(\gamma_{RD} + C)}{\gamma_{RD}} \right\} f_{\gamma_{RD}}(\gamma_{RD}) d\gamma_{RD} \end{aligned}$$

$$\begin{aligned}
&= 1 - \zeta \sum_{p=1}^{N_R} \sum_{s=0}^{p-1} \sum_{k=0}^N \sum_{n=0}^s \frac{\varphi_k A_R C^{s-n} \gamma^s \exp\left(-\frac{\gamma}{\lambda_{SR}}\right)}{\lambda_{SR}^s n! (s-n)!} \\
&\quad \times \int_0^\infty x^{\eta-1} G_{1,0}^{0,1} \left[ \frac{\lambda_{SR}}{C\gamma} x \middle| \begin{matrix} 1 \\ - \end{matrix} \right] G_{0,1}^{1,0} \left[ \mu x^{\frac{2}{r}} \middle| \begin{matrix} - \\ 0 \end{matrix} \right] dx \\
&= 1 - \zeta \underbrace{\sum_{k=0}^N \sum_{p=1}^{N_R} \sum_{s=0}^{p-1} \sum_{n=0}^s}_{\triangleq \sum_F} \Xi \gamma^{s+\eta} \exp\left(-\frac{\gamma}{\lambda_{SR}}\right) G_{0,r+2}^{r+2,0} [\delta \gamma^2 |_{K_1}] \\
&= 1 - \zeta \sum_F \gamma^{s+\eta} \exp\left(-\frac{\gamma}{\lambda_{SR}}\right) G_{0,r+2}^{r+2,0} [\delta \gamma^2 |_{K_1}], \tag{11}
\end{aligned}$$

where  $\eta = n - s + \frac{k+1}{r}$ ,  $\Xi = \frac{r^{0.5} 2^{-\eta-0.5} \varphi_k A_R C^{s-n+\eta}}{(2\pi)^{0.5r} \lambda_{SR}^{s+\eta} n! (s-n)!}$ ,  $\delta = \frac{\mu^r C^2}{4r' \lambda_{SR}^2}$ , and  $K_1 = [\Delta(r, 0), \Delta(2, -\eta)]$ .

## 2.2 Variable-Gain Relaying

For the scenarios that  $R$  has the CSI of  $S - R$  link, then  $R$  can use the appropriate gain to invert the fading effect of the  $S - R$  link while limiting the output power at  $R$  when the fading amplitude of the first hop is low. This scheme is also called as CSI-assisted relaying [34]. In this case, the received SNR at  $D$  is able to be approximately achieved by [10]

$$\gamma_{eq}^V \cong \min(\gamma_{SR}, \gamma_{RD}). \tag{12}$$

Then the CDF of  $\gamma_{eq}^V$  is obtained as

$$\begin{aligned}
F_{\gamma_{eq}^V}(\gamma) &= F_{\gamma_{SR}}(\gamma) + F_{\gamma_{RD}}(\gamma) - F_{\gamma_{SR}}(\gamma) F_{\gamma_{RD}}(\gamma) \\
&= 1 + \sum_{p=1}^{N_R} \sum_{s=0}^{p-1} \frac{A_R}{\lambda_{SR}^s s!} \gamma^s \exp\left(-\frac{\gamma}{\lambda_{SR}}\right) \left( \zeta \sum_{k=0}^N \tau_k G_{1,2}^{1,1} \left[ \mu \gamma^{\frac{2}{r}} \middle| \begin{matrix} 1 \\ \nu_{k,0} \end{matrix} \right] - Z_0^{PE} \right). \tag{13}
\end{aligned}$$

## 3. Secrecy Outage Probability Analysis

The SOP of mixed RF-FSO systems is obtained as [24]

$$\begin{aligned}
P_{out}(R_s) &= \Pr\{C_s(\gamma_{eq}, \gamma_{SE}) \leq R_s\} \\
&= \Pr\{\gamma_{eq} \leq \Theta \gamma_{SE} + \Theta - 1\} \\
&= \int_0^\infty F_{eq}(\Theta \gamma_{SE} + \Theta - 1) f_{\gamma_{SE}}(\gamma_{SE}) d\gamma_{SE}, \tag{14}
\end{aligned}$$

where  $\Theta = e^{R_s}$ .

Based on what we have known, the closed-form expression for (14) is not available due to the shift in the Meijer's  $G$ -function. In this section, we make use of the method used in [27], [35]–[38] and consider the bound of the SOP as

$$\begin{aligned}
P_{out}(R_s) &= \Pr\{\gamma_{eq} \leq \Theta \gamma_{SE} + \Theta - 1\} \\
&\geq P_{out}^L(R_s) = \Pr\{\gamma_{eq} \leq \Theta \gamma_{SE}\} \\
&= \int_0^\infty F_{\gamma_{eq}}(\Theta \gamma) f_{\gamma_{SE}}(\gamma) d\gamma. \tag{15}
\end{aligned}$$

### 3.1 Fixed-Gain Relaying

By placing (3) and (11) into (15), utilizing of (8) of [35] and (21) of [39], we obtain

$$\begin{aligned}
 P_{out}^{L,F}(R_s) &= \int_0^\infty F_{\gamma_{sq}^F}(\Theta\gamma) f_{\gamma_E}(\gamma) d\gamma \\
 &= 1 - \zeta \sum_F \sum_{q=1}^{N_E} \frac{\Theta^{s+\eta} A_E}{\Gamma(q) \lambda_E^q} \int_0^\infty \gamma^{s+\eta+q-1} \exp(-\phi_1 \gamma) G_{0,r+2}^{r+2,0}[\delta \Theta^2 \gamma^2 |_{K_1}] d\gamma \\
 &= 1 - \zeta \sum_F \sum_{q=1}^{N_E} \frac{2^{s+\eta+q-0.5} \Theta^{s+\eta} A_E}{(2\pi)^{0.5} \Gamma(q) \lambda_E^q} \phi_1^{-(s+\eta+q)} G_{2,r+2}^{r+2,2} \left[ \frac{4\delta \Theta^2}{\phi_1^2} \middle|_{K_2} \right], \quad (16)
 \end{aligned}$$

where  $\phi_1 = \frac{\Theta}{\lambda_{SR}} + \frac{1}{\lambda_{SE}}$  and  $K_2 = [\Delta(2, 1 - (s + \eta + q))]$ .

Since only the part of Meijer's G-function in (16) depends on  $\mu_r$ ,  $\delta \rightarrow 0$  as  $\lambda_{RD} \rightarrow \infty$ . Then, using (9.303) in [32] and  $\lim_{z \rightarrow 0^+} {}_p F_q(a, b, z) = 1$  [40], we can obtain the asymptotic SOP in this case as

$$P_{out}^{L,F,\infty}(R_s) = 1 - \zeta \sum_F \sum_{q=1}^{N_E} \frac{2^{s+\eta+q-0.5} \Theta^{s+\eta} A_E}{(2\pi)^{0.5} \Gamma(q) \lambda_E^q} \phi_1^{-(s+\eta+q)} \Lambda_1, \quad (17)$$

where

$$\Lambda_1 = \sum_{t=1}^{r+2} \left( \frac{4\delta \Theta^2}{\phi_1^2} \right)^{K_{1,t}} \left( \prod_{m=1, m \neq t}^{r+2} \Gamma(K_{1,m} - K_{1,t}) \prod_{m=1}^2 \Gamma(1 + K_{1,t} - K_{2,m}) \right)$$

and  $K_{m,n}$  stands for the  $n$ -th-term of  $K_m$ .

### 3.2 Variable-Gain Relaying

By placing (3) and (13) into (15) and utilizing (8) of [35], (21) of [39], and (3.326.2) of [32], we get

$$\begin{aligned}
 P_{out}^{L,V}(R_s) &= \int_0^\infty F_{\gamma_{sq}^V}(\Theta\gamma) f_{\gamma_E}(\gamma) d\gamma \\
 &= 1 + \sum_{\rho=1}^{N_R} \sum_{s=0}^{\rho-1} \sum_{q=1}^{N_E} \frac{A_R A_E \Theta^s}{\Gamma(q) \lambda_E^q \lambda_R^s s!} \phi_1^{-s-q} \\
 &\quad \times \left( \zeta \sum_{k=0}^N \frac{2^{s+q-0.5} \tau_k r^{\frac{k}{2}}}{(2\pi)^{0.5r}} G_{r,r+2}^{r,r+2} \left[ \frac{4\mu^r \Theta^2}{r^r \phi_1^2} \middle|_{K_4} \right] - (s+q-1)! Z_0^{PE} \right), \quad (18)
 \end{aligned}$$

where  $K_3 = [\Delta(r, 1), \Delta(2, 1 - s - q)]$  and  $K_4 = [\Delta(r, \nu_k), \Delta(r, 0)]$ .

Similarly with (17), we can obtain the asymptotic SOP with variable-gain scheme as

$$P_{out}^{L,V,\infty}(R_s) = 1 + \sum_{\rho=1}^{N_R} \sum_{s=0}^{\rho-1} \sum_{q=1}^{N_E} \frac{A_R A_E \Theta^s \phi_1^{-s-q}}{\Gamma(q) \lambda_E^q \lambda_R^s s!} \left( \zeta \sum_{k=0}^N \frac{2^{s+q-0.5} \tau_k r^{\frac{k}{2}} \Lambda_2}{(2\pi)^{0.5r}} - (s+q-1)! Z_0^{PE} \right), \quad (19)$$

where  $\Lambda_2 = \sum_{t=1}^r \frac{\prod_{m=1, m \neq t}^r \Gamma(K_{4,m} - K_{4,t}) \prod_{m=1}^{r+2} \Gamma(1 + K_{4,t} - K_{3,m})}{\prod_{m=r+1}^{2r} \Gamma(1 + K_{4,t} - K_{4,m})} \left( \frac{4\mu^r \Theta^2}{r^r \phi_1^2} \right)^{K_{4,t}}$ .

## 4. Numerical Results

In this part, some representative results are presented to explain the behavior of SOP with respect to the relaying schemes, pointing error, detection techniques, and the accuracy of the channel estimations on the secrecy outage performance of mixed RF-FSO systems with imperfect CSI. We set  $N_R = 3$ ,  $N_E = 2$ ,  $C = 1$ ,  $\rho_{SR} = \rho_{SE} = \rho_{RF}$ , and  $R_s = 0.1$  bit/s/Hz. One can find that the analytical

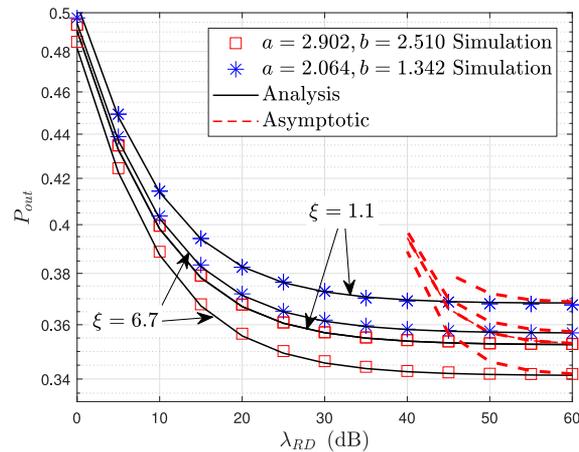


Fig. 3. SOP for different  $\xi$  with fixed-gain relaying,  $r = 2$ ,  $\rho_{RF} = \rho_{RD} = 0.5$ ,  $\lambda_{SR} = 10$  dB, and  $\lambda_{SE} = 0$  dB.

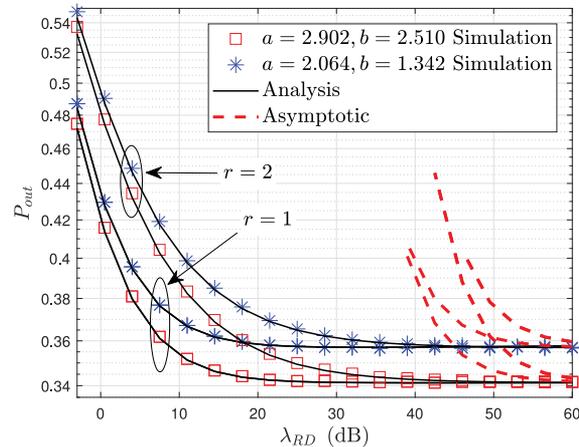


Fig. 4. SOP for different  $r$  with fixed-gain relaying,  $\xi = 6.7$ ,  $\rho_{RF} = \rho_{RD} = 0.5$ ,  $\lambda_{SR} = 10$  dB, and  $\lambda_{SE} = 0$  dB.

curves tightly approach the simulation results throughout all the figures. Furthermore, the secrecy outage performance aggravates due to the imperfect CSI.

Figs. 3–6 present the SOP with fixed-gain relaying scheme versus  $\lambda_{RD}$  for various  $\xi$ ,  $r$ ,  $\rho_{RF}$ , and  $\rho_{RD}$ , respectively. We can observe from Figs. 3 and 4 that the mixed RF-FSO systems in the cases with high  $\xi$  or less  $r$  are more secure than that with less  $\xi$  or high  $r$ . This is because that less  $\xi$  means higher pointing errors and HD detection technology can achieve better SNR at destinations compared with IM/DD. As observed from Figs. 5 and 6, one can find that imperfect CSI exhibits important influence on SOP and large  $\rho_{RF}$  or  $\rho_{RD}$  will lead to better secrecy performance since large correlation coefficient means more accurate channel estimation. Compared with  $\rho_{RF}$ , the influence of  $\rho_{RD}$  on SOP are more brutal since FSO link only influences the SNR at the destination while  $\rho_{RF}$  affects the SNR at both  $D$  and  $E$ . Moreover, as  $\lambda_{RD}$  increases, the effect of detection technology on secrecy performance becomes negligible, as testified in Fig. 5. The SOP with fixed-gain relaying scheme mainly depends on the pointing error parameter, the fading parameters of FSO link (if the channel estimation error of FSO link is lower) and the correlation coefficients of channels.

Figs. 7–10 present the SOP with variable-gain relaying scheme for various  $\xi$ ,  $r$ ,  $\rho_{RF}$ , and  $\rho_{RD}$ , respectively. As illustrated in Figs. 7–9, we are able to discover that  $\xi$ ,  $r$ , and  $\rho_{RD}$  exhibit similar effect on the SOP with fixed-gain relaying scheme in Figs. 3–5. However,  $\rho_{RF}$  shows different effect

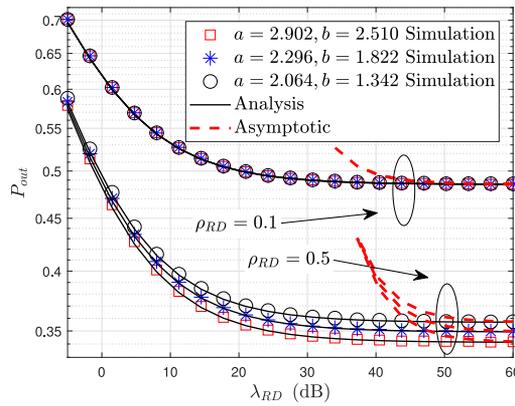


Fig. 5. SOP for different  $\rho_{RD}$  with fixed-gain relaying,  $r = 2$ ,  $\xi = 6.7$ ,  $\rho_{RF} = 0.5$ ,  $\lambda_{SR} = 10$  dB, and  $\lambda_{SE} = 0$  dB.

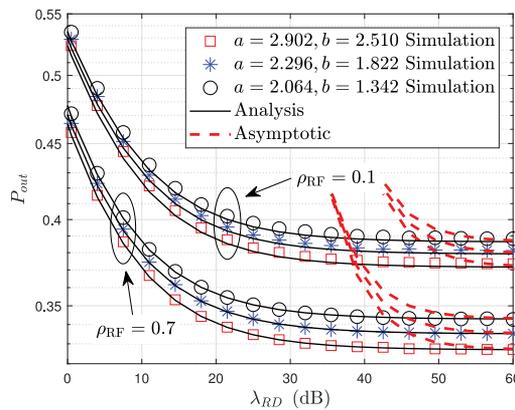


Fig. 6. SOP for different  $\rho_{RF}$  with fixed-gain relaying,  $r = 2$ ,  $\xi = 6.7$ ,  $\rho_{RD} = 0.5$ ,  $\lambda_{SR} = 10$  dB, and  $\lambda_{SE} = 0$  dB.

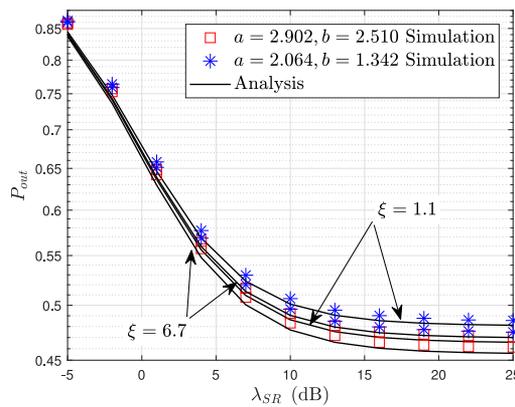


Fig. 7. SOP for different  $\xi$  with variable-gain relaying scheme,  $r = 2$ ,  $\rho_{RF} = \rho_{RD} = 0.5$ ,  $\lambda_{RD} = 10$  dB, and  $\lambda_{SE} = 0$  dB.

on the SOP with fixed-gain relaying scheme. It is shown in Fig. 10 that the secrecy performance with less  $\rho_{RF}$  outperforms that with larger  $\rho_{RF}$  in the high- $\lambda_{SR}$  region. This is because the SNR of  $R - D$  link is smaller than that of  $S - R$  link in the high- $\lambda_{SR}$  region, and then FSO link becomes dominant in  $S - R - D$  link. Small  $\rho_{RF}$  will lead to low SNR at  $E$  but does barely influence the SNR of FSO link. Thus the secrecy performance can be improved.

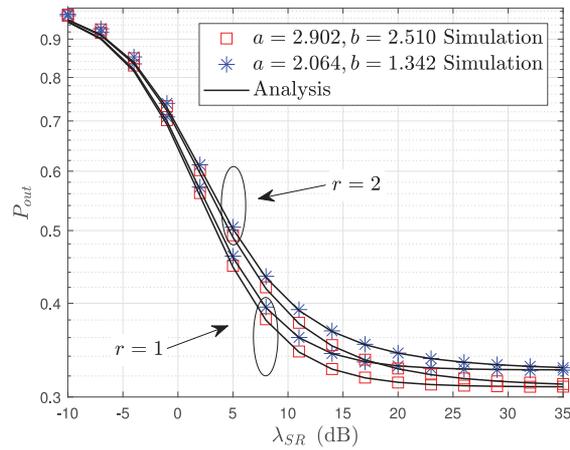


Fig. 8. SOP for different  $r$  with variable-gain relaying scheme,  $\xi = 6.7$ ,  $\rho_{RF} = \rho_{RD} = 0.5$ ,  $\lambda_{RD} = 10$  dB, and  $\lambda_{SE} = 0$  dB.

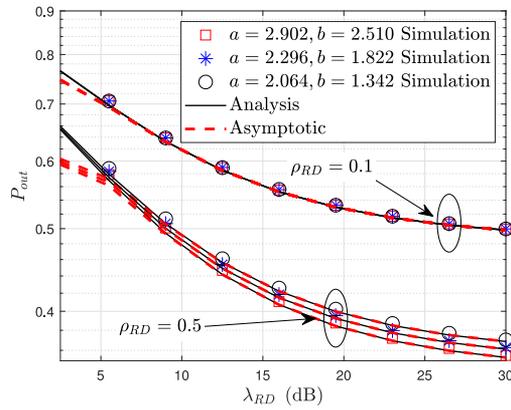


Fig. 9. SOP for different  $\rho_{RD}$  with variable-gain relaying scheme,  $r = 2$ ,  $\xi = 6.7$ ,  $\rho_{RF} = 0.5$ ,  $\lambda_{SR} = 10$  dB, and  $\lambda_{SE} = 0$  dB.

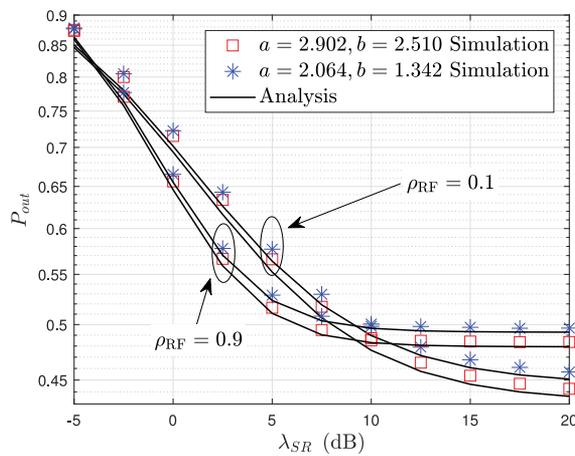


Fig. 10. SOP for different  $\rho_{RF}$  with variable-gain relaying scheme,  $r = 2$ ,  $\xi = 6.7$ ,  $\rho_{RD} = 0.5$ ,  $\lambda_{RD} = 10$  dB, and  $\lambda_{SE} = 0$  dB.

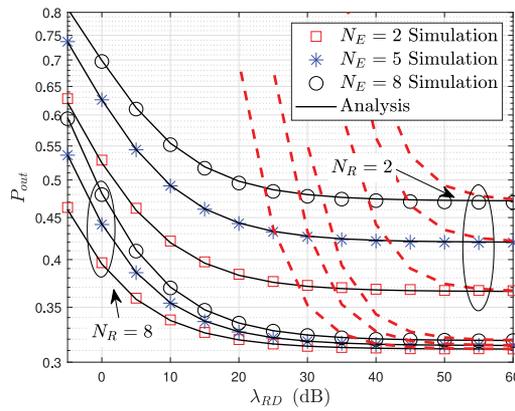


Fig. 11. SOP for different  $N_R$  with fixed-gain relaying,  $r = 2$ ,  $\xi = 6.7$ ,  $a = 2.902$ ,  $b = 2.510$ ,  $\rho_{RF} = \rho_{RD} = 0.5$ ,  $\lambda_{SR} = 10$  dB, and  $\lambda_{SE} = 0$  dB.

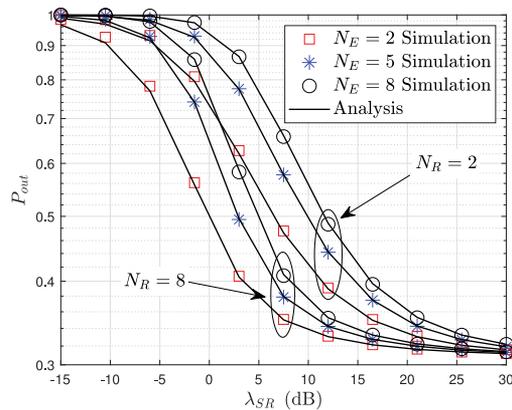


Fig. 12. SOP for different  $N_R$  with fixed-gain relaying,  $r = 2$ ,  $\xi = 6.7$ ,  $a = 2.902$ ,  $b = 2.510$ ,  $\rho_{RF} = \rho_{RD} = 0.5$ ,  $\lambda_{RD} = 10$  dB, and  $\lambda_{SE} = 0$  dB.

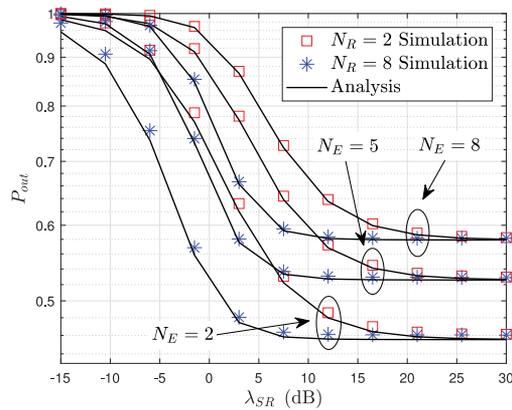


Fig. 13. SOP for different  $N_R$  with variable-gain relaying scheme,  $r = 2$ ,  $\xi = 6.7$ ,  $a = 2.902$ ,  $b = 2.510$ ,  $\rho_{RF} = \rho_{RD} = 0.5$ ,  $\lambda_{SR} = 10$  dB, and  $\lambda_{SE} = 0$  dB.

Figs. 11–13 present the SOP with different  $N_R$  and  $N_E$ , respectively. It is noted that large  $N_R$  or small  $N_E$  will improve the secrecy performance of mixed systems because more antennas can realize more diversity gains at destinations. An interesting phenomenon can be found from Fig. 14 that the SOP with variable-gain relaying scheme only depends on the number of antennas at  $E$

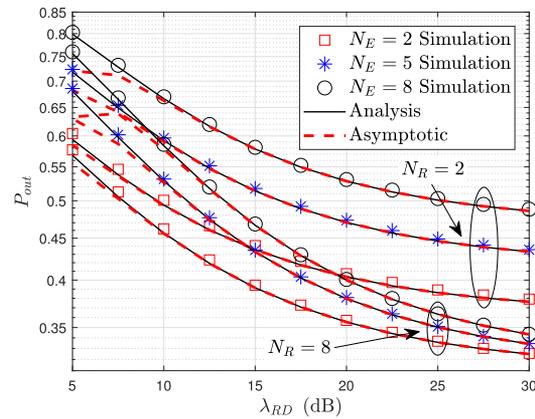


Fig. 14. SOP for different  $N_E$  with variable-gain relaying scheme,  $r = 2$ ,  $\xi = 6.7$ ,  $a = 2.902$ ,  $b = 2.510$ ,  $\rho_{RF} = \rho_{RD} = 0.5$ ,  $\lambda_{RD} = 10$  dB, and  $\lambda_{SE} = 0$  dB.

when  $\lambda_{SR}$  become larger, since the FSO link becomes dominant for the SNR at  $D$ . Then  $N_R$  almost does not influence the SOP.

## 5. Conclusion

In this paper, we investigated the effects of imperfect CSI for the RF link and the FSO link, misalignment, different detection schemes, and multi-antenna techniques on the secrecy performance of mixed RF-FSO systems. The closed-form expressions for the lower bound and asymptotic SOP were obtained. The results show that the secrecy outage performance of mixed RF-FSO systems degrades because of the imperfect CSI. Furthermore, the SOP of mixed RF-FSO systems depends on the fading parameters of FSO links and the pointing error in high-SNR region of FSO link.

## References

- [1] X. Li, J. Xiao, and J. Yu, "Long-distance wireless mm-wave signal delivery at W-band," *J. Lightw. Technol.*, vol. 34, no. 2, pp. 661–668, Jan. 2016.
- [2] X. Li, J. Yu, and J. Xiao, "Demonstration of ultra-capacity wireless signal delivery at W-band," *J. Lightw. Technol.*, vol. 34, no. 1, pp. 180–187, Jan. 2016.
- [3] X. Li *et al.*, "Delivery of 54-Gb/s 8QAM W-band signal and 32-Gb/s 16 QAM K-band signal over 20-km SMF-28 and 2500-m wireless distance," *J. Lightw. Technol.*, vol. 36, no. 1, pp. 50–56, Jan. 2018.
- [4] A. Mansour, R. Mesleh, and M. Abaza, "New challenges in wireless and free space optical communications," *Opt. Laser. Eng.*, vol. 89, pp. 95–108, Feb. 2017.
- [5] M. A. Khalighi and M. Uysal, "Survey on free space optical communication: A communication theory perspective," *IEEE Commun. Surveys Tuts.*, vol. 16, no. 4, pp. 2231–2258, Fourth Quarter 2014.
- [6] E. Lee, J. Park, D. Han, and G. Yoon, "Performance analysis of the asymmetric dual-hop relay transmission with mixed RF/FSO links," *IEEE Photon. Technol. Lett.*, vol. 23, no. 21, pp. 1642–1644, Nov. 2011.
- [7] I. S. Ansari, F. Yilmaz, and M. S. Alouini, "Impact of pointing error on the performance of mixed RF/FSO dual-hop transmission systems," *IEEE Wireless Commun. Lett.*, vol. 2, no. 3, pp. 351–354, Jun. 2013.
- [8] E. Zedini, I. S. Ansari, and M.-S. Alouini, "Performance analysis of mixed Nakagami- $m$  and Gamma-Gamma dual-hop FSO transmission systems," *IEEE Photon. J.*, vol. 7, no. 1, Feb. 2015, Art. no. 7900120.
- [9] J. Zhang, L. Dai, Y. Zhang, and Z. Wang, "Unified performance analysis of mixed radio frequency/free-space optical dual-hop transmission systems," *J. Lightw. Technol.*, vol. 33, no. 11, pp. 2286–2293, Jul. 2015.
- [10] E. Zedini, H. Soury, and M. S. Alouini, "On the performance analysis of dual-hop mixed FSO/RF systems," *IEEE Trans. Wireless Commun.*, vol. 15, no. 5, pp. 3679–3689, May 2016.
- [11] E. Soleimani-Nasab and M. Uysal, "Generalized performance analysis of mixed RF/FSO cooperative systems," *IEEE Trans. Wireless Commun.*, vol. 15, no. 1, pp. 714–727, Jan. 2016.
- [12] H. Samimi and M. Uysal, "End-to-end performance of mixed RF/FSO transmission systems," *IEEE J. Opt. Commun. Netw.*, vol. 5, no. 11, pp. 1139–1144, Nov. 2013.
- [13] L. Yang, M. O. Hasna, and X. Gao, "Performance of mixed RF/FSO with variable gain over generalized atmospheric turbulence channels," *IEEE J. Sel. Areas Commun.*, vol. 33, no. 9, pp. 1913–1924, Sep. 2015.
- [14] L. Yang, M. O. Hasna, and I. S. Ansari, "Unified performance analysis for multiuser mixed  $\eta-\mu$  and  $\mathcal{M}$ -distribution dual-hop RF/FSO systems," *IEEE Trans. Commun.*, vol. 65, no. 8, pp. 3601–3613, Aug. 2017.

- [15] P. V. Trinh, T. C. Thang, and A. T. Pham, "Mixed mmWave RF/FSO relaying systems over generalized fading channels with pointing errors," *IEEE Photon. J.*, vol. 9, no. 1, Feb. 2016, Art. no. 5500414.
- [16] J. Zhao, S.-H. Zhao, W.-H. Zhao, and K.-F. Chen, "Performance analysis for mixed FSO/RF Nakagami- $m$  and Exponentiated Weibull dual-hop airborne systems," *Opt. Commun.*, vol. 392, pp. 294–299, Jun. 2017.
- [17] G. T. Djordjevic, M. I. Petkovic, A. M. Cvetkovic, and G. K. Karagiannidis, "Mixed RF/FSO relaying with outdated channel state information," *IEEE J. Sel. Areas Commun.*, vol. 33, no. 9, pp. 1935–1948, Sep. 2015.
- [18] M. I. Petkovic, A. M. Cvetkovic, G. T. Djordjevic, and G. K. Karagiannidis, "Partial relay selection with outdated channel state estimation in mixed RF/FSO systems," *J. Lightw. Technol.*, vol. 33, no. 13, pp. 2860–2867, Jul. 2015.
- [19] A. M. Salhab, "Performance of multiuser mixed RF/FSO relay networks with generalized order user scheduling and outdated channel information," *Arab. J. Sci. Eng.*, vol. 40, no. 9, pp. 2671–2683, Jul. 2015.
- [20] A. M. Salhab, F. S. Al-Qahtani, R. M. Radaideh, S. A. Zummo, and H. Alnuweiri, "Power allocation and performance of multiuser mixed RF/FSO relay networks with opportunistic scheduling and outdated channel information," *J. Lightw. Technol.*, vol. 34, no. 13, pp. 3259–3272, Jul. 2016.
- [21] N. Varshney and M. Parul Puri, "Performance analysis of decode-and-forward-based mixed MIMO-RF/FSO cooperative systems with source mobility and imperfect CSI," *J. Lightw. Technol.*, vol. 35, no. 11, pp. 2070–2077, Jun. 2017.
- [22] M. Petkovic, G. T. Djordjevic, and I. B. Djordjevic, "Analysis of mixed RF/FSO system with imperfect CSI estimation," in *Proc. 19th Int. Conf. Transparent Opt. Netw.*, Girona, Spain, Jul. 2017, pp. 1–7.
- [23] J. Feng and X. Zhao, "Performance analysis of OOK-based FSO systems in Gamma-Gamma turbulence with imprecise channel models," *Opt. Commun.*, vol. 402, pp. 340–348, Nov. 2017.
- [24] M. Bloch, J. Barros, M. R. D. Rodrigues, and S. W. McLaughlin, "Wireless information-theoretic security," *IEEE Trans. Inf. Theory*, vol. 54, no. 6, pp. 2515–2534, Jun. 2008.
- [25] A. H. A. El-Malek, A. M. Salhab, S. A. Zummo, and M.-S. Alouini, "Security-reliability trade-off analysis for multiuser SIMO mixed RF/FSO relay networks with opportunistic user scheduling," *IEEE Trans. Wireless Commun.*, vol. 15, no. 9, pp. 5904–5918, Sep. 2016.
- [26] A. H. A. El-Malek, A. M. Salhab, S. A. Zummo, and M.-S. Alouini, "Effect of RF interference on the security-reliability trade-off analysis of multiuser mixed RF/FSO relay networks with power allocation," *J. Lightw. Technol.*, vol. 35, no. 9, pp. 1490–1505, May 2017.
- [27] H. Lei, Z. Dai, I. S. Ansari, K.-H. Park, G. Pan, and M.-S. Alouini, "On secrecy performance of mixed RF-FSO systems," *IEEE Photon. J.*, vol. 9, no. 4, Aug. 2017, Art. no. 7904814.
- [28] M. Gans, "The effect of Gaussian error in maximal ratio combiners," *IEEE Trans. Commun. Technol.*, vol. 19, no. 4, pp. 492–500, Aug. 1971.
- [29] G. Pan *et al.*, "On secrecy performance of MISO SWIPT systems with TAS and imperfect CSI," *IEEE Trans. Commun.*, vol. 64, no. 9, pp. 3831–3843, Sep. 2016.
- [30] H. Lei, J. Zhang, K.-H. Park, I. S. Ansari, G. Pan, and M.-S. Alouini, "Secrecy performance analysis of SIMO underlay cognitive radio systems with outdated CSI," *IET Commun.*, vol. 11, no. 12, pp. 1961–1969, Sep. 2017.
- [31] H. Zhao, Y. Tan, G. Pan, and Y. Chen, "Ergodic secrecy capacity of MRC/SC in SIMO wiretap systems with imperfect CSI," *Frontier Inf. Technol. Electron. Eng.*, vol. 18, no. 4, pp. 578–590, Apr. 2017.
- [32] I. Gradshteyn and I. Ryzhik, *Table of Integrals, Series and Products*, 7th ed. San Diego, CA, USA: Academic, 2007.
- [33] I. S. Ansari, F. Yilmaz, and M. S. Alouini, "Performance analysis of FSO links over unified Gamma-Gamma turbulence channels," in *Proc. IEEE 81st Veh. Technol. Conf.* Glasgow, U.K., May 2015, pp. 1–5.
- [34] M. O. Hasna and M.-S. Alouini, "A performance study of dual-hop transmissions with fixed gain relays," *IEEE Trans. Wireless Commun.*, vol. 3, no. 6, pp. 1963–1968, Nov. 2004.
- [35] H. Lei, C. Gao, Y. Guo, and G. Pan, "On physical layer security over generalized Gamma fading channels," *IEEE Commun. Lett.*, vol. 19, no. 7, pp. 1257–1260, Jul. 2015.
- [36] H. Lei, I. S. Ansari, C. Gao, Y. Guo, G. Pan, and K. Qaraqe, "Physical layer security over generalized- $K$  fading channels," *IET Commun.*, vol. 10, no. 16, pp. 2233–2237, Nov. 2016.
- [37] H. Lei, C. Gao, I. S. Ansari, Y. Guo, G. Pan, and K. Qaraqe, "On physical layer security over SIMO generalized- $K$  fading channels," *IEEE Trans. Veh. Technol.*, vol. 65, no. 9, pp. 7780–7785, Sep. 2016.
- [38] H. Lei, I. S. Ansari, C. Gao, Y. Guo, G. Pan, and K. A. Qaraqe, "Secrecy performance analysis of single-input multiple-output generalized- $K$  fading channels," *Frontier Inf. Technol. Electron. Eng.*, vol. 17, no. 10, pp. 1074–1084, Oct. 2016.
- [39] V. S. Adamchik and O. I. Marichev, "The algorithm for calculating integrals of hypergeometric type functions and its realization in reduce system," in *Proc. Int. Symp. Symbolic Algebraic Comput.* Tokyo, Japan, 1990, pp. 212–224.
- [40] M. Di Renzo, A. Guidotti, and G. E. Corazza, "Average rate of downlink heterogeneous cellular networks over generalized fading channels: A stochastic geometry approach," *IEEE Trans. Commun.*, vol. 61, no. 7, pp. 3050–3071, Jul. 2013.